Concentration matters: different stomatal CO_2-responses at sub-ambient and above-ambient CO_2 levels

Hanna Hõrak*, Kaspar Koolmeister*, Ebe Merilo, Hannes Kollist

Author affiliation: University of Tartu, Institute of Technology, Nooruse 1, 50411, Tartu, Estonia

*These authors contributed equally

Corresponding author contact: Hanna Hõrak, hanna.horak@ut.ee

Abstract

Stomatal pores, formed of paired guard cells, mediate CO_2 uptake for photosynthesis and water loss via transpiration in plants. Globally rising atmospheric CO_2 concentration triggers stomatal closure, contributing to increased leaf temperature and reduced nutrient uptake due to lower transpiration rate[1]. Hence, it is important to understand the signalling pathways that control elevated CO_2-induced stomatal closure to identify targets for breeding climate-ready crops. CO_2-induced stomatal closure can be studied by increasing CO_2 concentration from ambient to above-ambient concentrations[2,3], or elevation of CO_2 levels from sub-ambient to above-ambient[4,5]. Previous experiments comparing ferns with angiosperms suggested that stomatal responses to CO_2 may be different, when changing CO_2 levels in the sub-ambient or above-ambient ranges[3,6]. Here, we set out to test this by comparing CO_2-induced stomatal closure in key guard cell signalling mutants in response to CO_2 elevation from 100 to 400 ppm or 400 to 800 ppm. We show that signalling components that contribute to CO_2-induced stomatal closure are different in the sub-ambient and above-ambient CO_2 levels, with guard cell slow-type anion channel SLAC1 involved mainly in above-ambient CO_2-induced stomatal closure.

Stomata open in response to reduced CO_2 concentration and close in response to elevated CO_2 levels to balance photosynthetic CO_2 uptake and water loss via transpiration. The drought-inducible plant hormone abscisic acid (ABA) is a key regulator of stomatal closure. The ABA-induced signalling cascade in stomatal guard cells is triggered by the binding of ABA to its receptors, the PYR/PYL/RCAR proteins[7,8], that then form ternary complexes with negative regulators of ABA signalling, the protein phosphatases of group 2C (PP2C)[9]. In the absence of ABA, PP2Cs suppress the activation of positive regulators of ABA signalling, the protein kinase OST1[10–13] and the leucine-rich receptor-like pseudokinase GHR1[14,15]. In the presence of ABA, PP2Cs are inactivated, OST1 and GHR1 are activated and trigger anion efflux through the central guard cell slow-type anion channel SLAC1[12,13,16–18]. Thus, the activation of slow-type anion channel SLAC1 is the crucial step for effective ABA-induced stomatal closure.

Stomatal closure induced by elevated CO_2 concentration has remained less well understood. Similar to ABA, the activation of SLAC1 is required for stomatal closure in response to CO_2[16,18]. Mutations in genes coding for ABA signal transduction pathway components, such as the ABA receptors[5,19,20], PP2C phosphatases[19], and SLAC1-activating proteins OST1[21] and GHR1[15,22], have also been shown to result in impaired CO_2-induced stomatal closure. These

data indicate that the ABA signal transduction pathway contributes to CO_2-induced stomatal closure.

Nevertheless, some signalling components are involved in stomatal response to CO_2 but not ABA. Plants deficient in the function of the carbonic anhydrases CA1 and CA4[23], the mitogen-activated protein kinase MPK12[24] and the kinase HT1[22,25,26] all have impaired CO_2-responses but close stomata in response to ABA. Recently, MPK12 and a highly similar mitogen-activated protein kinase, MPK4, were shown to inhibit the activity of the HT1 kinase which in turn influenced activation of the SLAC1 anion channel by OST1 and GHR1[22,24,27]. This indicates the presence of a CO_2-specific branch of guard cell signal transduction pathways that is not required for ABA responses.

To understand the molecular mechanisms of CO_2-induced stomatal closure, it is important to define, what we mean by stomatal response to CO_2. Experiments assessing CO_2-induced stomatal closure have been carried out in different ways. In some studies, CO_2-induced stomatal closure is defined as a process that occurs, when CO_2 concentration is increased from ambient to above-ambient levels[2,3]. In others, a change from sub-ambient to above-ambient CO_2 concentration is used to trigger CO_2-induced stomatal closure[4,5]. Data from previous studies comparing CO_2-responses in ferns and angiosperms suggests that stomatal responses to CO_2 are different, when changing CO_2 levels in the sub-ambient or above-ambient ranges[3,6]. Thus, to understand stomatal regulation by CO_2, it is important to clarify, what do we talk about, when we talk about stomatal response to CO_2. Whether the underlying molecular mechanisms of stomatal closure caused by elevation of CO_2 concentration in the sub-ambient and above-ambient concentration ranges are different, has not been addressed.

We analysed stomatal responses to CO_2 in the sub-ambient and above-ambient concentration ranges in the model plant *Arabidopsis thaliana* to clarify whether these responses are controlled by the same regulators or display distinct underlying mechanisms. To this end, we used two types of experimental setups (Figure 1). In both types of experiments, we first reduced CO_2-levels from ambient 400 to 100 ppm to induce stomatal opening. Subsequently, CO_2 was either elevated from 100 to 400 ppm, and then from 400 to 800 ppm (Figure 1a), or alternatively directly from 100 to 800 ppm (Figure 1b). This approach allowed us to analyse three types of CO_2-induced stomatal closure: transition from 100 to 400 ppm (from here on referred to as 100-400), from 400 to 800 ppm (400-800), and from 100 to 800 ppm (100-800) of CO_2. Reaction kinetics of these responses were clearly different for wild type Col-0 plants. Stomatal closure induced by changing CO_2 from 100 to 400 ppm had the slowest reaction kinetics (rate constant $k = 0{,}026\ min^{-1}$) and 400 to 800 ppm closure had the fastest reaction kinetics ($k = 0.062\ min^{-1}$, Figure 1a). Stomatal closure induced by 100 to 800 ppm CO_2 transition is a mixture of 100 to 400 ppm and 400 and 800 ppm responses as also reflected in its intermediate reaction kinetics ($k = 0.038\ min^{-1}$, Figure 1b). The clearly different kinetics of these CO_2 responses suggest that underlying mechanisms could be regulated by different components.

To address the underlying mechanisms of CO_2-induced stomatal closure at different CO_2 transitions we studied plants deficient either in guard cell anion channel SLAC1 and its activation (*slac1-3*, *ghr1-3*, *ost1-3*) or in the CO_2-specific stomatal signalling branch regulated

by MPK12 and HT1 kinases (*mpk12-4*, *ht1-2*, *ht1-8D*) and carbonic anhydrases CA1 and CA4 (*ca1 ca4*) that convert CO_2 to bicarbonate. All studied mutants, except *ht1-2*, opened stomata at CO_2 transition from 400 to 100 ppm, although the responses of *ht1-8D*, *mpk12-4* and *ca1ca4* mutants were slower and smaller in magnitude compared to wild-type plants, as described before[22–25] (Figure 2a, f and Figure 3a, d). The 100-400 and 400-800 [CO_2] transitions revealed differences in sub-ambient and above-ambient CO_2-induced stomatal closure responses between SLAC1 and related mutants and plants deficient in CO_2-specific branch of stomatal signalling. We discuss these differences in terms of how fast stomata closed (k-values of fitted exponential functions, where appropriate) and what was the magnitude of response (reduction of stomatal conductance in absolute units).

In response to the 100-400 transition, the *slac1-3* and *ghr1-3* mutants closed their stomata with relatively fast exponential kinetics (Figure 2a); although the response was slower than in wild-type (Figure 2b), it was similar to wild-type in magnitude for *slac1-3* and close to that in *ghr1-3* (Figure 2c), indicating that SLAC1 and GHR1 are not of major importance in CO_2-induced stomatal closure at sub-ambient 100-400 CO_2 shifts. On the other hand, both SLAC1 and GHR1 were crucial for stomatal response to above-ambient CO_2 levels: *slac1-3* had slow, linear closure response of small magnitude and although *ghr1-3* had relatively fast closure response to the 400-800 transition, it was very low in magnitude (Figure 2a, d, e). The *ost1-3* mutant showed slow, linear response to both 100-400 and 400-800 transitions, indicating a regulatory role for the OST1 kinase in stomatal CO_2-responses across varying CO_2 concentration ranges. As SLAC1 is not the sole substrate of the OST1 kinase[28], it is likely that other OST1 targets are involved in CO_2-induced stomatal closure at sub-ambient CO_2 levels.

All the CO_2-signalling mutants, except *mpk12-4*, showed either no response (*ht1-2*, *ht1-8D*) or slow response with linear kinetics and small magnitude (*ca1ca4*) in response to 100-400 transition (Figure 2f, h). The response of *mpk12-4* to the 100-400 transition was exponential but significantly reduced in magnitude (Figure 2f-h). To the 400-800 transition, *ht1* mutants were again unresponsive, whereas *mpk12-4* and *ca1ca4* plants closed their stomata with exponential kinetics; their closure response was slower than in wild-type, but larger in magnitude (Figure 2f, i, j). Together, these data suggest that HT1 is crucial to initiate stomatal closure in response to CO_2 irrespective of CO_2 levels, whereas MPK12 function is more important at sub-ambient CO_2 concentrations. The carbonic anhydrases are needed at sub-ambient CO_2 levels to ensure fast stomatal closure in response to CO_2 elevation, whereas their role becomes less important in the 400-800 transition. This may be explained by increased nonenzymatic bicarbonate formation at higher CO_2 levels, rendering carbonic anhydrases less important.

In experiments where CO_2 concentrations were changed directly from 100 ppm to 800 ppm, the differences in responses that were detected for 100-400 and 400-800 transitions shown in Figure 2, were masked (Figure 3). Both *slac1-3* and *ost1-3* showed similar slow, non-exponential stomatal closure, whereas *ghr1-3* plants closed stomata as fast as wild-type plants but to a lower magnitude that was comparable with *slac1-3* and *ost1-3* (Figure 3a-c). Thus, by such an experimental set-up the important role for SLAC1 and GHR1 specifically in above-ambient CO_2-induced stomatal closure was not clear. The *ht1* mutants were insensitive to CO_2 shift from

100 to 800, as expected, whereas *mpk12-4* mutants had slower response of smaller magnitude compared to wild-type plants (Figure 3d-f). The *ca1ca4* mutants closed stomata slower but to the same extent as wild-type plants (Figure 3d-f). Thus, this experimental set-up did not allow to detect a more prominent role for MPK12 and carbonic anhydrases at sub-ambient CO_2 levels that was clear from experiments addressing the 100-400 and 400-800 transitions separately (Figure 2). In many cases the stomatal response to CO_2 elevation is studied by increasing CO_2 concentration from sub-ambient to above-ambient levels. Our experiments indicate that this can confound the interpretation of the results; and highlight the importance of experimental set-up, when studying and trying to understand the molecular mechanisms of stomatal response to elevated CO_2 concentration.

Here we show that stomatal closure in response to an increase in CO_2 concentration, which occurs both at sub-ambient and above-ambient CO_2 concentration ranges, comprises two different underlying processes. The CO_2-induced stomatal closure at a transition from ambient to above-ambient CO_2 levels displays fastest reaction kinetics and requires the activation of guard cell anion channel SLAC1 (Figure 2a-e), just like the ABA signal transduction pathway[16,18]. Conversely, the CO_2 specific carbonic anhydrases and the MPK12-HT1 signalling pathway have a major role when CO_2 levels change in the sub-ambient range (Figure 2f-j), albeit they also contribute to above-ambient CO_2-induced stomatal closure[22–24,27].

The mechanisms of CO_2-responses in the sub-ambient range of CO_2 concentrations, including stomatal opening response at low CO_2 levels, remain largely uncharacterised. During active photosynthesis, CO_2 concentrations in the intercellular air spaces, where CO_2 is perceived by the plant[29], are below ambient. Therefore, adequate and efficient responsiveness of plant stomata in this CO_2 concentration range is especially important to maximise photosynthetic efficiency. On the other hand, in the context of increasing global CO_2 levels and changing climate, understanding the molecular mechanisms of CO_2-induced stomatal closure, when CO_2 concentration rises above the current ambient levels, is of special interest. From the perspective of breeding water use efficient, but productive crops for the future climates, it is important to clearly define and differentiate the distinct processes underlying stomatal responses to CO_2, and to study them by experimental approaches that help to disentangle their molecular mechanisms.

Methods

Plant lines and growth conditions

Arabidopsis thaliana accession Col-0 and the following mutants in the same genetic background were used for experiments: *slac1-3*[16], *ost1-3*[30], *ghr1-3*[15], *ht1-2*[25], *ht1-8D*[22], *mpk12-4*[24], *ca1ca4*[23]. Plants were grown in 4:2:3 v/v peat:vermiculite:water mixture at 12/12 photoperiod with 150 μmol m^{-2} s^{-1} light in controlled-environment growth cabinets (AR-66LX; Percival Scientific; MCA1600, Snijders Scientific) at 70% relative humidity and day-time temperature of 23°C and night-time temperature 18°C. Plant age at experiment time was ~25 days.

Gas-exchange measurements

Measurements of stomatal conductance were carried out with a temperature-controlled custom-built gas-exchange device[3,31]. Plants were inserted into measurement cuvettes and allowed to acclimate for 1-2 hours at ~70% relative humidity, 24°C air temperature and 400 ppm CO_2. When stomatal conductance had stabilised, CO_2 concentration was reduced to 100 ppm for 2 hours. Thereafter, CO_2 concentration was either increased to 400 ppm and then to 800 ppm or directly from 100 ppm to 800 ppm; stomatal conductances were followed for 2 hours in each condition (Figure 1).

Data analysis

Magnitude of stomatal closure response was calculated as the difference in stomatal conductance between last time point before treatment and at the end of 2 hours of treatment at a given CO_2 level. Response curves were classified as exponential and non-exponential, the latter mostly comprising linear response curves. Response rate constants (k-values) were calculated by fitting exponential functions to response curves that behaved exponentially with GraphPad Prism 8.0.1. One-way ANOVA with Tukey *post hoc* test was used for statistical analysis as indicated in the figure legends, $p < 0.05$ were considered statistically significant. Statistical analyses were carried out with Past 4.0[32].

References

1. Ainsworth, E. A. & Long, S. P. 30 years of free-air carbon dioxide enrichment (FACE): What have we learned about future crop productivity and its potential for adaptation? *Glob. Change Biol.* **27**, 27–49 (2021).
2. Franks, P. J. & Britton-Harper, Z. J. No evidence of general CO_2 insensitivity in ferns: one stomatal control mechanism for all land plants? *New Phytol.* **211**, 819–827 (2016).
3. Hõrak, H., Kollist, H. & Merilo, E. Fern Stomatal Responses to ABA and CO_2 Depend on Species and Growth Conditions. *Plant Physiol.* **174**, 672–679 (2017).
4. Azoulay-Shemer, T. *et al.* Guard cell photosynthesis is critical for stomatal turgor production, yet does not directly mediate CO_2- and ABA-induced stomatal closing. *Plant J.* **83**, 567–581 (2015).
5. Chater, C. *et al.* Elevated CO_2-Induced Responses in Stomata Require ABA and ABA Signaling. *Curr. Biol.* **25**, 2709–2716 (2015).
6. Brodribb, T. J., McAdam, S. A. M., Jordan, G. J. & Feild, T. S. Evolution of stomatal responsiveness to CO_2 and optimization of water-use efficiency among land plants. *New Phytol.* **183**, 839–847 (2009).
7. Ma, Y. *et al.* Regulators of PP2C Phosphatase Activity Function as Abscisic Acid Sensors. *Science* **324**, 1064–1068 (2009).
8. Park, S.-Y. *et al.* Abscisic Acid Inhibits Type 2C Protein Phosphatases via the PYR/PYL Family of START Proteins. *Science* **324**, 1068–1071 (2009).
9. Melcher, K. *et al.* A gate–latch–lock mechanism for hormone signalling by abscisic acid receptors. *Nature* **462**, 602–608 (2009).
10. Mustilli, A.-C., Merlot, S., Vavasseur, A., Fenzi, F. & Giraudat, J. Arabidopsis OST1 Protein Kinase Mediates the Regulation of Stomatal Aperture by Abscisic Acid and Acts Upstream of Reactive Oxygen Species Production. *Plant Cell* **14**, 3089–3099 (2002).
11. Fujii, H. *et al. In vitro* Reconstitution of an ABA Signaling Pathway. *Nature* **462**, 660–664 (2009).
12. Geiger, D. *et al.* Activity of guard cell anion channel SLAC1 is controlled by drought-stress signaling kinase-phosphatase pair. *Proc. Natl. Acad. Sci.* **106**, 21425–21430 (2009).

13. Lee, S. C., Lan, W., Buchanan, B. B. & Luan, S. A protein kinase-phosphatase pair interacts with an ion channel to regulate ABA signaling in plant guard cells. *Proc. Natl. Acad. Sci.* **106**, 21419–21424 (2009).
14. Hua, D. *et al.* A Plasma Membrane Receptor Kinase, GHR1, Mediates Abscisic Acid- and Hydrogen Peroxide-Regulated Stomatal Movement in *Arabidopsis*. *Plant Cell Online* **24**, 2546–2561 (2012).
15. Sierla, M. *et al.* The Receptor-like Pseudokinase GHR1 Is Required for Stomatal Closure. *Plant Cell* **30**, 2813–2837 (2018).
16. Vahisalu, T. *et al.* SLAC1 is required for plant guard cell S-type anion channel function in stomatal signalling. *Nature* **452**, 487–491 (2008).
17. Vahisalu, T. *et al.* Ozone-triggered rapid stomatal response involves the production of reactive oxygen species, and is controlled by SLAC1 and OST1. *Plant J.* **62**, 442–453 (2010).
18. Negi, J. *et al.* CO_2 regulator SLAC1 and its homologues are essential for anion homeostasis in plant cells. *Nature* **452**, 483–486 (2008).
19. Merilo, E. *et al.* PYR/RCAR Receptors Contribute to Ozone-, Reduced Air Humidity-, Darkness-, and CO_2-Induced Stomatal Regulation. *Plant Physiol.* **162**, 1652–1668 (2013).
20. Dittrich, M. *et al.* The role of Arabidopsis ABA receptors from the PYR/PYL/RCAR family in stomatal acclimation and closure signal integration. *Nat. Plants* **5**, 1002–1011 (2019).
21. Xue, S. *et al.* Central functions of bicarbonate in S-type anion channel activation and OST1 protein kinase in CO_2 signal transduction in guard cell. *EMBO J.* **30**, 1645–1658 (2011).
22. Hõrak, H. *et al.* A Dominant Mutation in the HT1 Kinase Uncovers Roles of MAP Kinases and GHR1 in CO_2-Induced Stomatal Closure. *Plant Cell* **28**, 2493–2509 (2016).
23. Hu, H. *et al.* Carbonic anhydrases are upstream regulators of CO_2-controlled stomatal movements in guard cells. *Nat. Cell Biol.* **12**, 87–93 (2010).
24. Jakobson, L. *et al.* Natural Variation in *Arabidopsis* Cvi-0 Accession Reveals an Important Role of MPK12 in Guard Cell CO_2 Signaling. *PLOS Biol.* **14**, e2000322 (2016).
25. Hashimoto, M. *et al.* Arabidopsis HT1 kinase controls stomatal movements in response to CO_2. *Nat. Cell Biol.* **8**, 391–397 (2006).
26. Hashimoto-Sugimoto, M. *et al.* Dominant and recessive mutations in the Raf-like kinase *HT1* gene completely disrupt stomatal responses to CO_2 in Arabidopsis. *J. Exp. Bot.* **67**, 3251–3261 (2016).
27. Tõldsepp, K. *et al.* Mitogen-activated protein kinases MPK4 and MPK12 are key components mediating CO2-induced stomatal movements. *Plant J.* **96**, 1018–1035 (2018).
28. Wang, P. *et al.* Mapping proteome-wide targets of protein kinases in plant stress responses. *Proc. Natl. Acad. Sci.* (2020) doi:10.1073/pnas.1919901117.
29. Mott, K. A. Do Stomata Respond to CO_2 Concentrations Other than Intercellular? *Plant Physiol.* **86**, 200–203 (1988).
30. Yoshida, R. *et al.* ABA-Activated SnRK2 Protein Kinase is Required for Dehydration Stress Signaling in *Arabidopsis*. *Plant Cell Physiol.* **43**, 1473–1483 (2002).
31. Kollist, T. *et al.* A novel device detects a rapid ozone-induced transient stomatal closure in intact Arabidopsis and its absence in abi2 mutant. *Physiol. Plant.* **129**, 796–803 (2007).
32. Hammer, O., Harper, D. A. T. & Ryan, P. D. PAST: Paleontological Statistics Software Package for Education and Data Analysis. *Palaeontol. Electron.* **4**, 10 (2001).

Acknowledgements

This work was supported by the Estonian Research Council grants PSG404 to H.H., Basic funding from the Institute of Technology and PRG719 to E.M. and PRG433 to H.K.; and European Regional Development Fund via Center of Excellence in Molecular Cell Engineering.

Author Contributions

H.H. designed the study, H.H., K.K. and E.M. performed experiments, H.H., K.K., E.M. and H.K. analysed data, H.H. and H.K. wrote the manuscript, all authors commented, edited and approved the final manuscript.

Competing Interests statement

The authors declare no competing interests.

Figure Legends

Figure 1. Kinetics of CO_2-induced stomatal closure in wild-type Arabidopsis.

Col-0 wild-type Arabidopsis stomatal response to elevation of CO_2 concentration **(a)** from 100 to 400 ppm and 400 to 800 ppm, **(b)** and from 100 to 800 ppm. Fitted k-values (rate constant) with 95% confidence intervals are shown next to respective response curves. Mean stomatal conductance ± SEM is shown. Sample size was 17 in **(a)** and 14 in **(b)**.

Figure 2. Stomatal responses to CO_2 concentration elevation from 100 to 400 ppm and 400 to 800 ppm are mediated by different regulators.

(a) and **(f)** Stomatal response to CO_2 concentration elevation from 100 to 400 ppm and 400 to 800 ppm, mean stomatal conductance ± SEM is shown. **(b, g)** and **(d, i)** Boxplot of fitted k-values (rate constants) of stomatal response to CO_2 concentration elevation from 100 to 400 ppm and 400 to 800 ppm respectively, linear responses are marked as NA (not applicable). **(c, h)** and **(e, j)** Boxplot of absolute stomatal closure (mmol m^{-2} s^{-1}) in response to CO_2 concentration elevation from 100 to 400 ppm and 400 to 800 ppm respectively. **(b-i)** and **(g-j)** Boxes represent 25-75 % quartiles and median as the horizontal line inside, whiskers indicate the smallest and largest values, points show individual plant values. Statistically significantly different groups are marked with different letters (One-way ANOVA with Tukey *post hoc* test). **(a-j)** Sample size was 17 for Col-0 and *ost1-3*; 7 for *ht1-2* and *ht1-8D*; 16 for *ghr1-3* and *slac1-3*, 10 for *ca1ca4* and 12 for *mpk12-4*.

Figure 3. Analysing stomatal response to CO_2-elevation from sub-ambient to above-ambient CO_2 levels masks underlying mechanisms.

(a) and **(d)** Stomatal responses to CO_2 concentration elevation from 100 to 800 ppm, mean stomatal conductance ± SEM is shown. **(b)** and **(e)** Boxplot of k-values (rate constants) during stomatal response to CO_2 concentration elevation from 100 to 800 ppm, linear responses are marked as NA (not applicable). **(c)** and **(f)** Boxplot of absolute stomatal closure (mmol m^{-2} s^{-1})

292 in response to CO_2 concentration elevation from 100 to 800 ppm. **(b, c, e, f)** Boxes represent
293 25-75 % quartiles and the median as horizontal line inside, whiskers indicate the smallest and
294 largest values, points show individual plant values. Statistically significantly different groups
295 are marked with different letters (One-way ANOVA with Tukey *post hoc* test). **(a-f)** Sample
296 size was 14 for Col-0; 6 for *ht1-2*; 7 for *ht1-8D*; 8 for *ghr1-3*, *mpk12-4* and *ost1-3*; 9 for *slac1-*
297 *3* and *ca1ca4*.

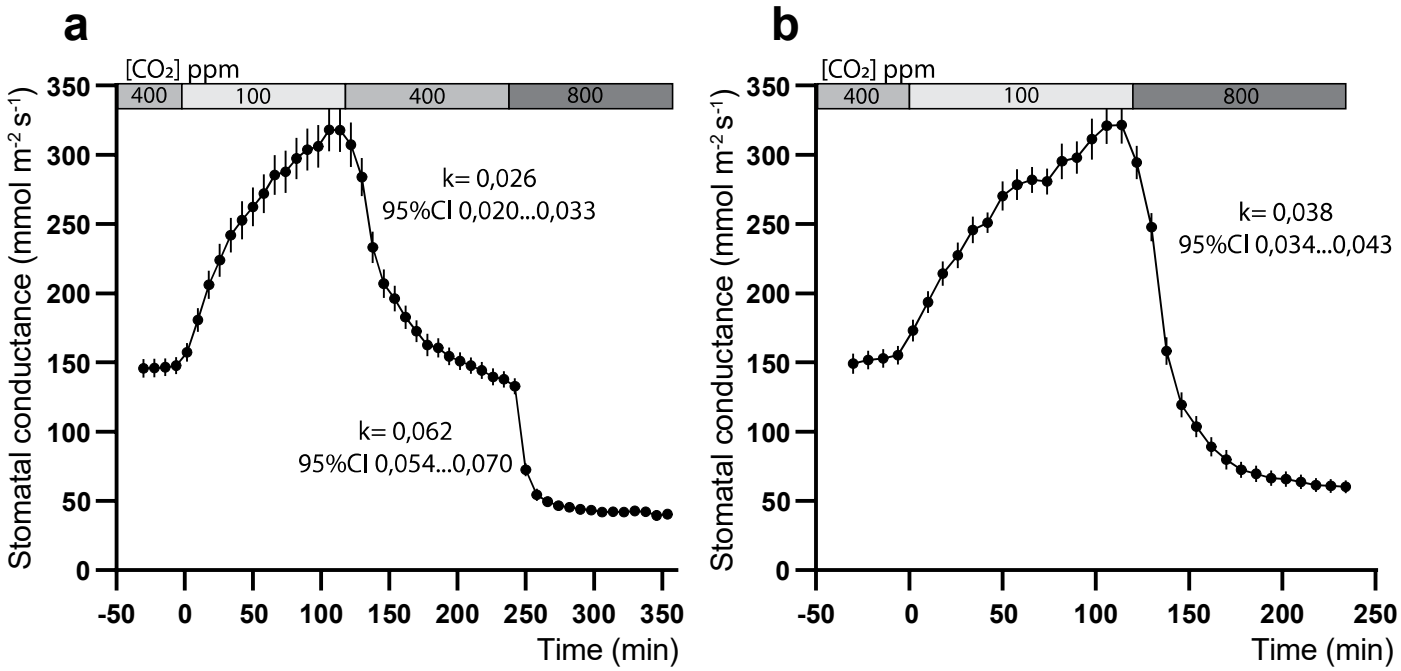

Figure 1. Kinetics of CO_2-induced stomatal closure in wild-type Arabidopsis.
Col-0 wild-type Arabidopsis stomatal response to elevation of CO_2 concentration **(a)** from 100 to 400 ppm and 400 to 800 ppm, **(b)** and from 100 to 800 ppm. Fitted k-values (rate constant) with 95% confidence intervals are shown next to respective response curves. Mean stomatal conductance ± SEM is shown. Sample size was 17 in **(a)** and 14 in **(b)**.

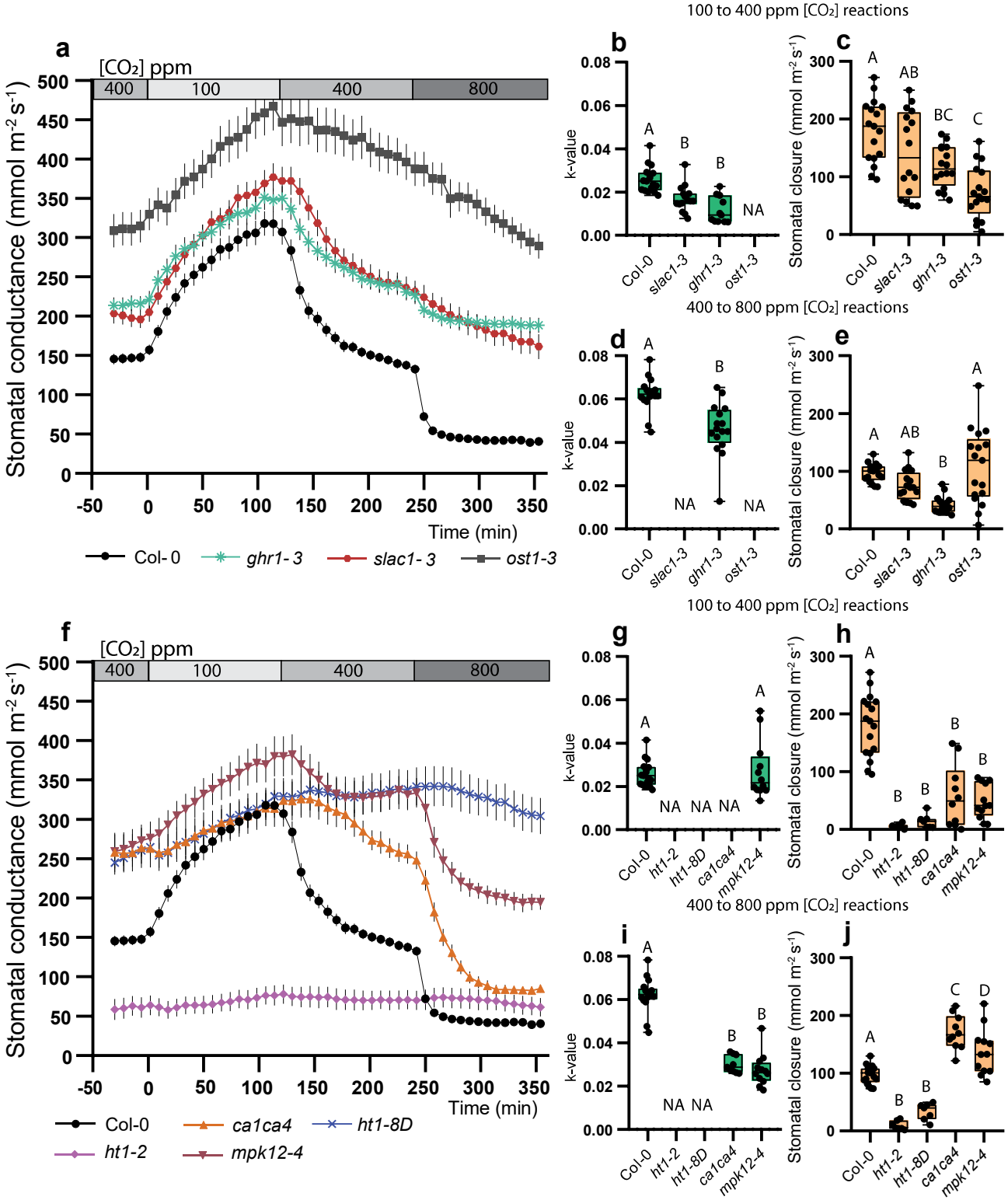

Figure 2. Stomatal responses to CO_2 concentration elevation from 100 to 400 ppm and 400 to 800 ppm are mediated by different regulators.

(a) and **(f)** Stomatal response to CO_2 concentration elevation from 100 to 400 ppm and 400 to 800 ppm, mean stomatal conductance ± SEM is shown. **(b, g)** and **(d, i)** Boxplot of fitted k-values (rate constants) of stomatal response to CO_2 concentration elevation from 100 to 400 ppm and 400 to 800 ppm respectively, linear responses are marked as NA (not applicable). **(c, h)** and **(e, j)** Boxplot of absolute stomatal closure (mmol m^{-2} s^{-1}) in response to CO_2 concentration elevation from 100 to 400 ppm and 400 to 800 ppm respectively. **(b-i)** and **(g-j)** Boxes represent 25-75 % quartiles and median as the horizontal line inside, whiskers indicate the smallest and largest values, points show individual plant values. Statistically significantly different groups are marked with different letters (One-way ANOVA with Tukey *post hoc* test). **(a-j)** Sample size was 17 for Col-0 and *ost1-3*; 7 for *ht1-2* and *ht1-8D*; 16 for *ghr1-3* and *slac1-3*, 10 for *ca1ca4* and 12 for *mpk12-4*.

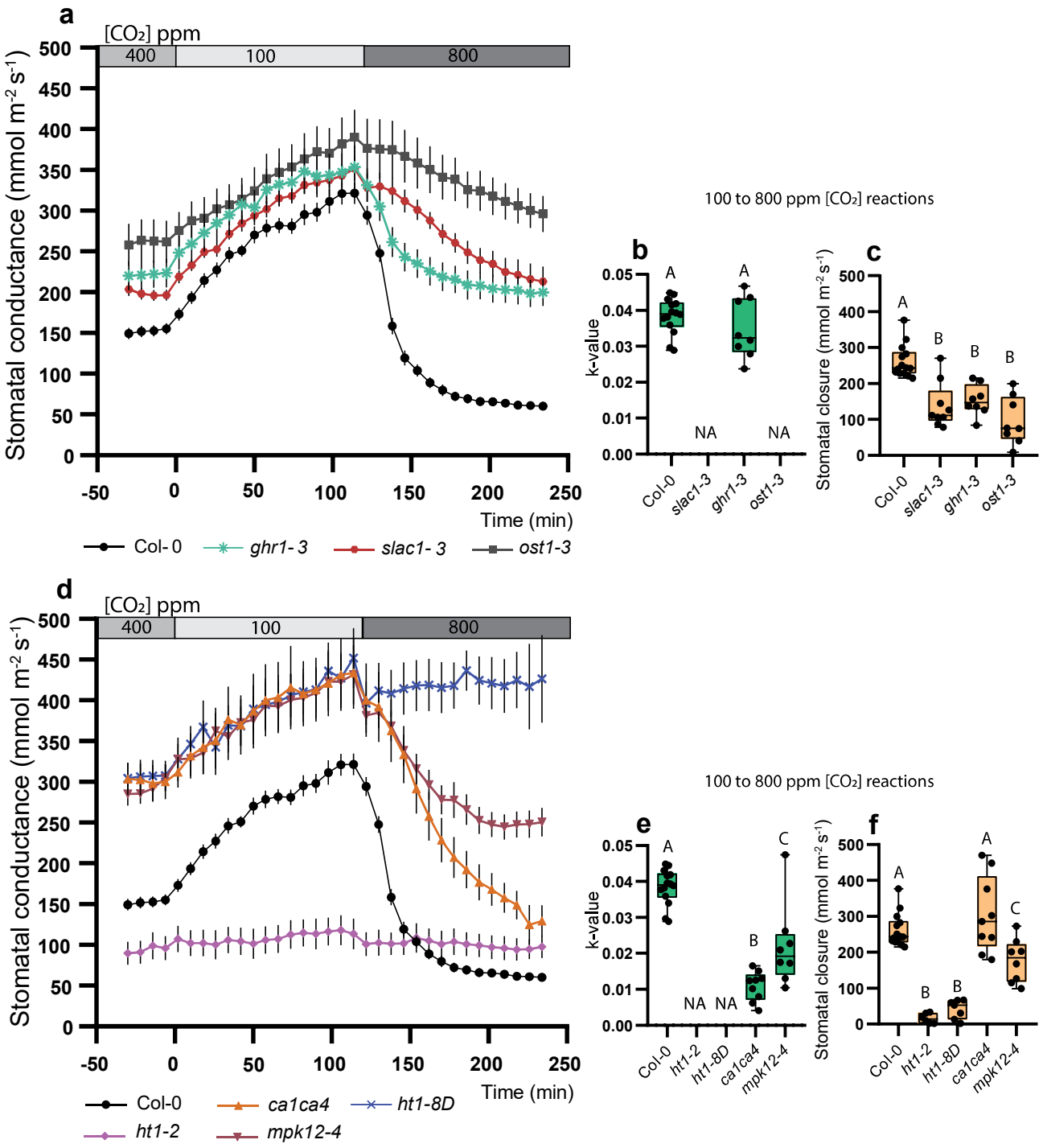

Figure 3. Analysing stomatal response to CO_2-elevation from sub-ambient to above-ambient CO2 levels masks underlying mechanisms.

(a) and **(d)** Stomatal responses to CO_2 concentration elevation from 100 to 800 ppm, mean stomatal conductance ± SEM is shown. **(b)** and **(e)** Boxplot of k-values (rate constants) during stomatal response to CO_2 concentration elevation from 100 to 800 ppm, linear responses are marked as NA (not applicable). **(c)** and **(f)** Boxplot of absolute stomatal closure (mmol m^{-2} s^{-1}) in response to CO_2 concentration elevation from 100 to 800 ppm. **(b, c, e, f)** Boxes represent 25-75 % quartiles and the median as horizontal line inside, whiskers indicate the smallest and largest values, points show individual plant values. Statistically significantly different groups are marked with different letters (One-way ANOVA with Tukey *post hoc* test). **(a-f)** Sample size was 14 for Col-0; 6 for *ht1-2*; 7 for *ht1-8D*; 8 for *ghr1-3*, *mpk12-4* and *ost1-3*; 9 for *slac1-3* and *ca1ca4*.